Title: Impact of polyplex micelles installed with cyclic RGD peptide as ligand on gene delivery to vascular lesions

Running title: **Gene delivery to vascular lesions**

Authors: **Hideo Kagaya[1,2] , Makoto Oba [3], Yutaka Miura [2], Hiroyuki Koyama [2], Takehiko Ishii [4], Tsuyoshi Takato [2], Kazunori Kataoka [5], Tetsuro Miyata 1**

[1] Division of Vascular Surgery, Department of Surgery, Graduate School of Medicine, The University of Tokyo, Bunkyo-ku, Tokyo, Japan
[2] Division of Tissue Engineering, The University of Tokyo, Bunkyo-ku, Tokyo, Japan
[3] Department of Molecular Medicinal Sciences, Graduate School of Biomedical Sciences, Nagasaki University, Nagasaki-shi, Japan
[4] Department of Bioengineering, Graduate School of Engineering, The University of Tokyo, Bunkyo-ku, Tokyo, Japan
[5] Department of Materials Engineering, Graduate School of Engineering, The University of Tokyo, Bunkyo-ku, Tokyo, Japan

Correspondence: **Hiroyuki Koyama, Division of Tissue Engineering, The University of Tokyo, 7-3-1 Hongo, Bunkyo-ku, Tokyo, 113-8655, Japan.**
E-mail: hkoyama-tky@umin.ac.jp
Telephone: +81-3-3815-5411 Fax: +81-3-3811-6822

Word count: **4729**

Abstract

Gene therapy is expected to open a new strategy for the treatment of refractory vascular diseases, so the development of appropriate gene vectors for vascular lesions is needed. To realize this requirement with a non-viral approach, cyclo(RGDfK) peptide (cRGD) was introduced to block copolymer, poly(ethylene glycol)-block-polycation carrying ethylenediamine units (PEG-PAsp(DET)). cRGD recognizes $\alpha_v\beta_3$ and $\alpha_v\beta_5$ integrins, which are abundantly expressed in vascular lesions. cRGD-conjugated PEG-PAsp(DET) (cRGD-PEG-PAsp(DET)) formed polyplex micelles through complexation with plasmid DNA (pDNA), and the cRGD-PEG-PAsp(DET) micelles achieved significantly more efficient gene expression and cellular uptake as compared with PEG-PAsp(DET) micelles in endothelial cells and vascular smooth muscle cells. Intracellular tracking of pDNA showed that cRGD-PEG-PAsp(DET) micelles were internalized via caveolae-mediated endocytosis, which is associated with a pathway avoiding lysosomal degradation, and that PEG-PAsp(DET) micelles were transported to acidic endosomes and lysosomes via clathrin-mediated endocytosis. Further, in vivo evaluation in rat carotid artery with a neointimal lesion revealed that cRGD-PEG-PAsp(DET) micelles realized sustained gene expression, while PEG-PAsp(DET) micelles facilitated rapid but transient gene expression. These findings suggest that introduction of cRGD to polyplex micelles might create novel and useful functions for gene transfer and contribute to the establishment of efficient gene therapy for vascular diseases.

Keywords: gene delivery; vascular lesion; neointimal hyperplasia; polyplex micelle; cyclo(RGDfK) peptide

Introduction

Therapeutic application of gene delivery techniques is expected to open a new strategy for the treatment of refractory vascular disease, and a variety of methods have been proposed for delivering therapeutic genes to vascular wall cells.[1,2] In these methods, viral vectors have been mostly utilized as the gene carrier, since gene transfer efficiency with viral vectors is generally superior to that of other non-viral methods. However, there are some limitations in the clinical application of viral vectors, the most critical of which might be the problem of safety due to antigenicity and oncogenicity.[3,4] These issues of viral vectors have impelled the development of non-viral vectors with safety and reasonable efficiency of gene transfer.[5,6] Polyplex and lipoplex systems, in which plasmid DNA (pDNA) forms a polyion complex with cationic polymers and cationic lipids, respectively, have been widely studied as conventional non-viral vectors.[7-10] It is known that polyplex and lipoplex potentially achieve desirable efficiency of gene transfer in vitro. However, positive charges on these vectors potentially induce cytotoxicity and nonspecific aggregation with plasma proteins, indicating that in vivo administration of these vectors might be considerably restricted.[11,12]

Polyplex micelles were developed to resolve these restrictions of non-viral vectors. They were constructed from newly synthesized block copolymer characterized by tandem alignment of a hydrophilic poly(ethylene glycol) (PEG) segment and a polycationic segment.[13-15] Then, a proper mixture of the block copolymer and pDNA potently forms stable polyplex micelles that possess a unique core-shell structure of a hydrophilic shell layer surrounding a polyplex core.[16,17] Because of the hydrophilic property of the PEG shell, the polyplex micelle minimizes nonspecific interactions with

various bio-components, realizing high biocompatibility and stability in vivo.[18-20] In previous studies, we also designed PEG-block-polycation carrying ethylenediamine units in the side chain (PEG-PAsp(DET)), and reported that polyplex micelles with PEG-PAsp(DET) accomplished appreciable gene transfer efficiency with low cytotoxicity.[20,21] After internalization of PEG-PAsp(DET) micelles into the intracellular compartment by endocytosis, the ethylenediamine units are expected to promote translocation of the polyplex micelles toward the cytoplasm due to endosomal membrane destabilization, resulting in improvement of gene transfer efficiency.[22,23] Furthermore, to increase cellular uptake of polyplex micelles, we recently attempted to introduce appropriate ligands into the surface of the polyplex micelles.[24-26] The installed ligands potently enhanced uptake into the targeted cells by inducing receptor-mediated endocytosis, while polyplex micelles without ligands were taken up only through adsorptive or fluid-phase endocytosis.

In the present study, cyclo(RGDfK) peptide (cRGD) was introduced to the PEG terminal of PEG-PAsp(DET) in order to function as a specific ligand on the surface of the polyplex micelle (Fig. 1). cRGD peptide selectively recognizes $\alpha_v\beta_3$ and $\alpha_v\beta_5$ integrins,[27] and previous studies showed that $\alpha_v\beta_3$ and $\alpha_v\beta_5$ are abundantly expressed on endothelial cells and smooth muscle cells in vascular lesions.[28-30] PEG-PAsp(DET) micelles installed with cRGD (cRGD-PEG-PAsp(DET) micelles) were applied to endothelial cells and vascular smooth muscle cells in vitro and also to rat carotid artery with neointimal hyperplasia, and the efficacy of gene transfer was evaluated as compared with that of ligand-free PEG-PAsp(DET) micelles.

Results

Expression of $\alpha_v\beta_3$ and $\alpha_v\beta_5$ integrins on HUVEC and VSMC

To evaluate the expression of $\alpha_v\beta_3$ and $\alpha_v\beta_5$ ingtegrins on vascular wall cells, flow cytometric analysis of human umbilical vein endothelial cells (HUVEC) and human vascular smooth muscle cells (VSMC) was carried out using FITC-labeled antibodies against $\alpha_v\beta_3$ and $\alpha_v\beta_5$. Flow cytometric analysis revealed considerable expression of $\alpha_v\beta_3$ and $\alpha_v\beta_5$ on HUVEC and VSMC as compared with control (Fig. 2a, b).

In vitro gene transfer to HUVEC and VSMC

The expression plasmid vector containing the luciferase gene was complexed with cRGD-PEG-PAsp(DET) at various N/P ratios, and applied to HUVEC or VSMC in vitro. Here, N/P ratio refers to the unit molar ratio of amino groups in the polymer to phosphate groups in the pDNA. Gene expression was assessed by measuring luciferase activity 24 hours later, and polyplex micelles with PEG-PAsp(DET) were utilized in the same manner as control. In gene transfer to HUVEC, luciferase activity after treatment with cRGD-PEG-PAsp(DET) micelles was significantly higher than that with PEG-PAsp(DET) micelles at N/P ratios of, 5 and 10 (Fig. 3a). At N/P ratios of 2, 20 and 30, no remarkable difference in luciferase activity was detected between cRGD-PEG-PAsp(DET) micelles and PEG-PAsp(DET) micelles, though the activity was appreciably high at N/P ratios of 20 and 30. In gene transfer to VSMC, cRGD-PEG-PAsp(DET) micelles showed significantly higher luciferase activity at N/P ratios of 4 and 5, as compared with PEG-PAsp(DET) micelles, while there was no difference in activity between the two types of micelles at N/P ratios of 2, 10 and 20 (Fig. 3b).

Cellular uptake of polyplex micelles

To assess uptake of cRGD-PEG-PAsp(DET) micelles into vascular cells in vitro, Cy5-labeled pDNA (Cy5-pDNA) was complexed with cRGD-PEG-PAsp(DET) at N/P ratio of 5, and administered to HUVEC or VSMC in vitro. Intensity of Cy5 incorporated into these cells was analyzed by flow cytometry at 0.5, 1, 3 and 6 hours after administration. PEG-PAsp(DET) micelles containing Cy5-pDNA were used as control. In both HUVEC and VSMC, the intracellular intensity of Cy5 after transfer with cRGD-PEG-PAsp(DET) micelles were significantly higher than that with PEG-PAsp(DET) micelles at all time points except 6 hours in VSMC (Fig. 4a, b).

Intracellular distribution of polyplex micelles

Other sets of cultured HUVEC and VSMC were also treated with cRGD-PEG-PAsp(DET) micelles or PEG-PAsp(DET) micelles containing Cy5-pDNA, and the intracellular distribution of Cy5-pDNA (red) was evaluated at 6 and 24 hours by confocal laser scanning microscopy (CLSM). Simultaneously, HUVEC and VSMC were stained with LysoTracker Green (green) to identify acidic endosomes and lysozomes, or cholera toxin subunit B (CT-B) Alexa Fluor 488 (green) for lipid rafts and caveosomes, and colocalization with incorporated Cy5-pDNA was quantified. In HUVEC, intracellular Cy5-pDNA after transfer with PEG-PAsp(DET) micelles considerably colocalized with LysoTracker Green as compared with that with cRGD-PEG-PAsp(DET) micelles at 6 and 24 hours after treatment (Fig. 5b). On the contrary, Cy5-pDNA after transfer with cRGD-PEG-PAsp(DET) micelles markedly colocalized with CT-B as compared with that with PEG-PAsp(DET) micelles (Fig. 5a).

These findings were statistically confirmed by quantitative analyses using colocalization ratio (Fig. 5c, d). The same experiments using VSMC showed similar results. Cy5-pDNA transferred with cRGD-PEG-PAsp(DET) micelles tended to colocalize with intracellular CT-B, and that with PEG-PAsp(DET) micelles tended to associate with LysoTracker Green at both 6 and 24 hours after application of micelles, which were confirmed by statistical analyses (Fig. 5e-h).

Gene transfer to neointimal lesion induced in rat carotid artery

Rat carotid artery was injured with a balloon catheter, which induced neointimal hyperplasia by 21 days after injury. Expression pDNA fused with luciferase gene was complexed with cRGD-PEG-PAsp(DET) at N/P ratio of 5, and polyplex micelles were administered into the carotid artery with neointima. The carotid arteries were sampled at 1, 2, 3 and 4 days after treatment, and luciferase activity of the carotids was measured to evaluate gene expression in the arteries. PEG-PAsp(DET) micelles complexed with luciferase pDNA (N/P ratio = 5) were applied in the same manner as control. In the carotid arteries subjected to cRGD-PEG-PAsp(DET) micelles, maximum activity of luciferase was observed at 2 days after application of micelles, and activity on day 3 and 4 was similar to that on day 1 (Fig. 6a). On the contrary, in the arteries treated with PEG-PAsp(DET) micelles, luciferase activity showed a maximum value on day 1, though only low level activity was detected on day 3 and 4. Statistical analyses showed that the day 1 activity of carotid samples treated with PEG-PAsp(DET) micelles was significantly higher than that with cRGD-PEG-PAsp(DET) micelles. However, on day 3 and 4, arterial samples after treatment with cRGD-PEG-PAsp(DET) micelles showed significantly high luciferase activity as compared with those after application of

PEG-PAsp(DET) micelles. There was no difference in values on day 2 between the two groups.

pDNA was also complexed with cRGD-PEG-PAsp(DET) or PEG-PAsp(DET) at N/P ratio of 20. The micelles were applied into carotid arteries with neointima in the same manner. In the carotid arteries subjected to cRGD-PEG-PAsp(DET) micelles and also those with PEG-PAsp(DET), luciferase measurement showed markedly low activity on day 2 and also day 3, which was significantly lower than that after application of micelles with N/P ratio of 5 (Fig. 6b, c).

In vivo uptake of polyplex micelles

To evaluate in vivo uptake of polyplex micelles in the rat carotid artery with neointima, Cy3-labeled pDNA was complexed with cRGD-PEG-PAsp(DET) or PEG-PAsp(DET) at N/P ratio of 5, and the micelles were administered into the arteries (Fig. 7). At 1 day after application of micelles, the carotid arteries were excised, and cross sections were analyzed with a fluorescence microscope. In carotid arteries subjected to cRGD-PEG-PAsp(DET) micelles, considerable diffuse fluorescence of Cy3 was observed in all of the neointimal layer, while scarce fluorescence was detected in arteries treated with PEG-PAsp(DET) micelles (Fig. 7a, b). Cy3 intensity in the neointima was quantified as fluorescence intensity index, and the index after treatment with cRGD-PEG-PAsp(DET) micelles was significantly higher than that with PEG-PAsp(DET) micelles (Fig. 7c).

Discussion

In the present study, cRGD peptide was introduced to the surface of polyplex micelles with PEG-PAsp(DET) as a specific ligand for $\alpha_v\beta_3$ and $\alpha_v\beta_5$, and its gene transfer efficacy to vascular wall cells and lesion-induced artery was analyzed in comparison with that of ligand-free PEG-PAsp(DET) micelles. PEG-PAsp(DET) micelles complexed with pDNA tightly pack the DNA into a dense shell layer of hydrophilic PEG, assuring high stability and biocompatibility in vivo.[16,17] Further, after cellular uptake by endocytosis, the ethylenediamine units of the polycation are potently protonated in the endosome and considered to promote desirable translocation toward the cytoplasm due to endosomal membrane destabilization.[22,23] Our previous study indeed showed that administration of PEG-PAsp(DET) micelles into rabbit carotid artery accomplished appreciable gene transfer to the artery without occlusion by thrombus formation.[20] In contrast, the same study revealed that polyplex made from polyethyleneimine markedly caused thrombus occlusion after intra-arterial application, indicating that positively charged polyplex potentially underwent aggregation with plasma proteins and blood cells. Since thrombus formation possibly interferes with the process of gene transfer and further impairs vascular functions, it appears necessary for gene vectors for the treatment of vascular diseases to possess non-thrombogenic properties, like PEG-PAsp(DET) micelles.

It is known that $\alpha_v\beta_3$ and $\alpha_v\beta_5$ integrins are expressed on various vascular cells such as endothelial cells, smooth muscle cells and macrophages, and that they play an important role in atherogenesis and formation of other vascular lesions, which was a rational basis for selection of cRGD peptide as a ligand of the gene vector for vascular lesions.[28,31-35] In the present study, HUVEC and VSMC were used for in vitro study. We

were initially concerned about the possibility that integrins expressed on HUVEC and VSMC markedly differed from those on endothelial cells and smooth muscle cells in vascular lesions in vivo, since neither of these cells was harvested from the diseased artery. However, flow cytometry revealed obvious expression of $\alpha_v\beta_3$ and $\alpha_v\beta_5$ on HUVEC and VSMC, indicating that these cells were appropriate for in vitro evaluation of the micelles.

In vitro study using the luciferase gene showed that gene expression after transfer with cRGD-PEG-PAsp(DET) micelles was significantly higher than that with PEG-PAsp(DET) micelles in both HUVEC and VSMC at low N/P ratios. This finding clearly demonstrated that introduction of cRGD potentially improved the gene expression efficiency of the micelles at low N/P ratios. We previously carried out gene transfer experiments using HeLa cells, which abundantly express $\alpha_v\beta_3$ and $\alpha_v\beta_5$, and reported similar improvement of gene expression after delivery with cRGD-fused polyplex micelles, while no improvement was detected in 293 cells expressing neither $\alpha_v\beta_3$ nor $\alpha_v\beta_5$.[36] One possible mechanism to explain the improvement might be that association of cRGD ligands with $\alpha_v\beta_3$ and $\alpha_v\beta_5$ integrins efficiently enhanced cellular uptake of polyplex micelles through receptor-mediated endocytosis. Indeed, in both HUVEC and VSMC, cellular uptake of Cy5-pDNA after treatment with cRGD-PEG-PAsp(DET) micelles (N/P = 5) was significantly higher than that with PEG-PAsp(DET) micelles (N/P = 5) at 0.5, 1 and 3 hours after treatment. A previous study using HeLa cells also showed that simultaneous administration of free cRGD peptides considerably reduced the improvement of gene transfer with cRGD-fused polyplex micelles, suggesting a contribution of receptor-mediated uptake due to cRGD ligands.[37] Another possible mechanism for the improved gene expression with

cRGD-PEG-PAsp(DET) micelles might be that cRGD ligands modulated intracellular trafficking after uptake of the polyplex micelles. In CLSM analyses of HUVEC and VSMC, pDNA transferred with cRGD-PEG-PAsp(DET) micelles tended to co-localize with lipid rafts and caveosomes, and pDNA after transfer with PEG-PAsp(DET) micelles tended to associate with acidic endosomes and lysosomes. Grosse et al. evaluated the cellular uptake of particles that were not installed with any ligands, and showed that the process of cellular uptake depended upon particle size; particles with >200 nm diameter were internalized by macropinocytosis, particles with 100-200 nm diameter by clathrin-mediated endocytosis, and particles <100 nm diameter by caveolae-mediated endocytosis.[38] The average diameter of cRGD-PEG-PAsp(DET) and PEG-PAsp(DET) micelles was around 100 nm, with a moderate distribution. Since PEG-PAsp(DET) micelles were particles without ligands, a main process in cellular uptake of PEG-PAsp(DET) micelles was then suspected to be clathrin-mediated endocytosis, and the principle components of the endocytic pathway are endosomes and lysozomes, supporting the CLSM findings on PEG-PAsp(DET) micelles. Meanwhile, previous studies showed that expression of $\alpha_v\beta_3$ integrins promoted cellular uptake via caveolae-mediated endocytosis, and that $\alpha_v\beta_5$ expression facilitated clathrin-mediated endocytosis.[39-41] Since the binding affinity of cRGD with $\alpha_v\beta_3$ is 10 times stronger than that with $\alpha_v\beta_5$, it might be reasonable that caveolae-mediated endocytosis was a dominant process in cellular uptake of cRGD-PEG-PAsp(DET) micelles.[42] In contrast to clathrin-mediated endocytosis, the internalization pathway via caveolae-mediated endocytosis is known to bypass degradative organelles and not to be associated with a decrease in pH. Therefore, it is possible that cRGD-PEG-PAsp(DET) micelles enabled avoidance of enzymatic degradation after internalization via caveolae-mediated

endocytosis, resulting in enhanced gene expression.

The principal aim of the present study was to evaluate gene transfer efficacy to vascular lesions using cRGD-PEG-PAsp(DET) micelles and PEG-PAsp(DET) micelles. Vascular lesions as the target of gene therapy are generally related to atherosclerosis or its associated diseases, and such lesions develop from the intimal layer of the arterial wall. Major cell components of intimal lesions are intimal SMC and monocytes/macrophages, and previous studies showed that the biological properties of these cells were markedly different from those of medial SMC and other cells in normal artery.[43,44] Thus, to develop gene transfer methods targeting vascular lesions, in vivo experiments must be carried out on artery with intimal lesions, not normal artery. In the present study, we induced neointimal hyperplasia in the rat carotid artery by balloon injury, and then administered polyplex micelles into the same artery, which might be an appropriate model to acquire highly reliable data on vascular gene transfer.

In vivo study using the luciferase gene showed that overall gene expression with the polyplex micelles at N/P ratio of 5 was markedly higher than that at N/P ratio of 20, and the time-course of gene expression revealed a clear contrast between the delivery with cRGD-PEG-PAsp(DET) micelles (N/P = 5) and that with PEG-PAsp(DET) micelles (N/P = 5). Namely, delivery with cRGD-PEG-PAsp(DET) micelles facilitated sustained gene expression, while that with PEG-PAsp(DET) micelles promoted rapid but transient expression of the transferred gene. The contrast in gene expression between these micelles could be explained by the difference in intracellular trafficking after endocytosis. Since cRGD peptide possesses high affinity with $\alpha_v\beta_3$, cRGD-PEG-PAsp(DET) micelles might be predominantly internalized through caveolae-mediated endocytosis, whereby the micelles undergo neither enzymatic

degradation nor pH decrease during intracellular trafficking.[45] The avoidance of enzymatic degradation potentially prolonged the half-life of pDNA in the cells, and then realized sustained expression of the transferred gene. The absence of a decrease in pH indicated that endosomal membrane destabilization was hardly caused by PAsp(DET) polycation of cRGD-PEG-PAsp(DET) micelles, which possibly delayed translocation of the gene toward the cytoplasm. The present study indeed showed that gene expression at 1 day after treatment with cRGD-PEG-PAsp(DET) micelles was considerably lower than that with PEG-PAsp(DET) micelles, although in vivo uptake of Cy3-pDNA at 1 day after treatment with cRGD-PEG-PAsp(DET) micelles was significantly superior to that with PEG-PAsp(DET) micelles. In contrast, PEG-PAsp(DET) micelles might be mostly internalized via clathrin-mediated endocytosis and then transported to the endosomes. A low pH in the endosomes potentially protonated some PEG-PAsp(DET) micelles and accelerated translocation of the gene toward the cytoplasm by endosomal membrane destabilization, which might promote rapid expression of the transferred gene. However, since other PEG-PAsp(DET) micelles were inevitably transported to the lysozomes and digested by enzymatic hydrolysis, gene expression might tend to be transient. We consider that such a difference in the gene expression pattern suggests the possibility of combined application of cRGD-PEG-PAsp(DET) and PEG-PAsp(DET) micelles. If both micelles were simultaneously administered to the targeted artery, it might be feasible to achieve rapid and sustained gene expression in the arterial wall.

In conclusion, polyplex micelles with cRGD-PEG-PAsp(DET) achieved significantly more_efficient gene expression and cellular uptake as compared with ligand-free PEG-PAsp(DET) micelles in both HUVEC and VSMC, which expressed $\alpha_v\beta_3$ and $\alpha_v\beta_5$ integrins. Tracer study of pDNA showed that cRGD-PEG-PAsp(DET)

micelles were internalized into HUVEC and VSMC via caveolae-mediated endocytosis, and that PEG-PAsp(DET) micelles were internalized via clathrin-mediated endocytosis. Further, in vivo evaluation in a rat carotid artery with neointimal hyperplasia revealed that cRGD-PEG-PAsp(DET) micelles realized sustained gene expression, while PEG-PAsp(DET) micelles facilitated rapid but transient gene expression. These findings demonstrated that cRGD-PEG-PAsp(DET) and PEG-PAsp(DET) micelles possessed different characters of gene expression in vivo and efficiently functioned as non-viral gene vectors for vascular lesions.

Materials and Methods

Synthesis of cRGD-PEG-PAsp(DET) and PEG-PAsp(DET)

Acetal-PEG-PAsp(DET) was prepared as previously reported. Briefly, β-benzyl-L-aspartate *N*-carboxyanhydride was polymerized in *N,N*-dimethylformamide/CH_2Cl_2 (1 : 10) at 35˚C by initiation from the primary amino group of acetal-PEG-NH_2 (Mw of PEG: 12,000 g/mol). Acetal-PEG-*b*-poly(β-benzyl L-aspartate) (acetal-PEG-PBLA) was recovered by precipitation in an excess amount of *n*-hexane/AcoEt (6 : 4), and the filtrate was dried in vacuo. The degree of polymerization of PBLA was calculated as 68 from the ^{1}H NMR spectrum (data not shown). The side-chain aminolysis reaction of PBLA was then performed by mixing with a 50-fold excess of diethylenetriamine (DET) in NMP at 0˚C to obtain acetal-PEG-PAsp(DET). Introduction of cRGD peptide (Peptide Institute, Osaka, Japan) into block copolymer was carried out as previously reported. Briefly, acetal-PEG-PAsp(DET) was added to cRGD peptide in 0.2 M AcOH buffer (pH 4.0)

and stirred at room temperature for 5 days. The reacted polymer was purified by dialysis with 0.01 N HCl and distilled water and lyophilized to obtain cRGD-PEG-PAsp(DET). The introduction rate of the cRGD peptide ligands was determined to be 45% from the ^{1}H NMR spectrum (data not shown).

Detection of $\alpha_v\beta_3$ and $\alpha_v\beta_5$ integrins on HUVEC and VSMC

HUVEC (Cambrex Corporation, East Rutherford, NJ), cultured in EBM-2 medium containing growth supplement (Lonza, Walkersville, MD), and human VSMC (Applied Cell Biology Research Institute, Kirkland, WA), cultured in CS-C medium (Applied Cell Biology Research Institute), were detached by trypsin treatment, and 5×10^5 cells were resuspended in 100 μL EBM-2 medium for HUVEC and CS-C medium for VSMC. FITC-labeled antibody against $\alpha_v\beta_3$ integrin, $\alpha_v\beta_5$ integrin, or mouse IgG (2 μg, Cosmo Bio Co., Ltd., Tokyo, Japan) was added to each cell suspension, followed by incubation on ice for 1 h in the dark. The cells were washed three times with cold medium and, after being resuspended in PBS, were analyzed by flow cytometry (BD LSR II instrument, BD Biosciences, Franklin Lakes, NJ). This experiment was performed twice.

Plasmids

Plasmid pCAccluc+ was constructed by inserting the recombinant luciferase gene (luc+) into the pCAGGS expression vector. Plasmids were grown in competent DH5α *E. coli* and purified with a QIAGEN HiSpeed Plasmid MaxKit (Germantown, MD). In order to analyze the localization of the transferred gene, pDNA was labeled with Cy5 or Cy3 (Label IT kits, Pierce Co., Inc., Rockford, IL).

Preparation of polyplex micelles

cRGD-PEG-PAsp(DET), PEG-PAsp(DET) and pDNA were separately dissolved in 10 mM Hepes buffer (pH 7.4). The polymer solution was added to a 2-fold excess volume of pDNA solution to form polyplex micelles at various N/P ratios, the residual molecular ratio of amino groups in the block copolymer to phosphate groups in pDNA.

In vitro gene transfer to HUVEC and VSMC

HUVEC or VSMC were seeded on 24-well culture plate (20,000 cells / well) and cultured overnight in 500 μL EBM-2 or CS-C medium, respectively. pCAccluc+ was complexed with cRGD-PEG-PAsp(DET) or PEG-PAsp(DET), and N/P ratios of the polyplex micelles were adjusted to 2, 5, 10, 20 and 30 for gene transfer to HUVEC, and 2, 4, 5, 10 and 20 for gene transfer to VSMC. After replacement with fresh culture medium, 30 μL micelle solution (33.3 μg pDNA / mL) was applied to each well (1 μg pDNA / well) (n =3) and incubated at 37˚C. At 24 h after application of micelle solution, the cells were lysed in 100 μL cell culture lysis reagent (Promega), and luciferase activity was evaluated using a Luciferase assay kit (Promega) and a Lumat LB9507 luminometer (Berthold Technologies, Bad Wildbad, Germany). The results were expressed as relative light units (RLU) per milligram of total protein measured using a Micro BCA protein assay reagent kit (Rockford).

Cellular uptake of polyplex micelles

HUVEC or VSMC was seeded on 6-well culture plates (100,000 cells / well) and incubated overnight in 2 mL of each medium. Cy5-pDNA was complexed with

cRGD-PEG-PAsp(DET) or PEG-PAsp(DET) at N/P ratio of 5, and 90 μL of each micelle solution (33.3 μg pDNA / mL) was applied to each well (3 μg pDNA / well) after replacement with fresh culture medium and incubated at 37˚C. At 0.5, 1, 3 and 6 h after application of micelle solution (n = 4), the medium was removed and the cells were washed 3 times with PBS. After detachment by trypsin, the cells were re-suspended in PBS and analyzed by flow cytometry.

Intracellular distribution of incorporated pDNA

HUVEC or VSMC were seeded on a 35-mm glass base dish (100,000 cells / dish, Iwaki, Tokyo, Japan) and incubated overnight in 2 mL of each medium. After medium change, 90 μL polyplex micelle (containing Cy5-pDNA) solution (N/P = 5, 33.3 μg pDNA / mL) was applied to a glass base dish, and incubated for 6 or 24 h (n = 3). The intracellular distribution of the polyplex micelles was observed with a confocal laser scanning microscope (CLSM) after staining acidic endosomes and lysosomes with LysoTracker Green (Molecular Probes, Eugene, OR), or lipid rafts and caveosomes with CT-B Alexa Fluor 488 (Molecular Probes). CLSM observation was performed using an LSM 510 (Carl Zeiss, Oberlochen, Germany) with a C-Apochromat 63× objective (Carl Zeiss) at a suitable excitation wavelength.

To evaluate the final destination of polyplex micelles, the rate of colocalization of Cy5-pDNA with LysoTracker Green or CT-B Alexa Fluor 488 was quantified. LysoTracker Green was used as a marker of late endosomes and lysosomes, and CT-B Alexa Fluor 488 was used as a marker of lipid rafts and caveosomes. Colocalization was quantified as follows:

$$\text{Colocalization ratio} = Pix_{colocalization} / Pix_{total}$$

where $Pix_{colocalization}$ represents the number of Cy5 pixels colocalizing with LysoTracker Green or CT-B Alexa Fluor 488, and Pix_{total} represents the number of all pixels in the cell.

Animal model and evaluation of gene expression efficiency

All animal experiments were approved by the Institutional Animal Care and Use Committee and conducted in conformity with institutional guidelines. SD rats (weight, 300-400 g: Kurea, Tokyo Japan) fed a normal diet were anesthetized by intraperitoneal injection of ketamine (75 mg/kg) and xylazine (10 mg/kg). A 2 Fr Fogarty balloon catheter (Baxter Healthcare, CA) was introduced through the first branch of the left external carotid artery and passed into the left common carotid artery. The balloon was inflated at physiological pressure and passed through the common carotid artery three times with constant rotation. At 21 days after balloon injury, polyplex micelles were administered into the common carotid artery, in which neointimal hyperplasia had been induced. pCAccluc+ was complexed with cRGD-PEG-PAsp(DET) or PEG-PAsp(DET) at N/P ratio of 5. Then, proximal sites of the common carotid artery and internal carotid artery were clamped with a vessel clip, and a PE-10 tube (Clay Adams) was introduced into the common carotid artery through the external carotid artery. After flashing with Ringer's solution, 200 μL of each micelle solution (20 mg pDNA / mL) was gently infused into the common carotid artery through the tube (4 mg pDNA). The distal common carotid artery was then clamped, and the common carotid artery was left for 20 min. The vessel clips of the carotid artery were then removed, and the arterial circulation was restored. Animals were sacrificed at 1, 2, 3 and 4 days after administration of micelles (n = 6-8), and the left common carotid artery was excised.

After removal of surrounding connective tissue, each sample was homogenized and lysed in 300 μl cell culture lysis reagent, and luciferase activity of each lysate was measured. Gene transfer efficiency was evaluated as the ratio of luciferase activity to the protein content. The results were expressed as RLU / mg protein.

Additionally, pCAccluc+ was also complexed with cRGD-PEG-PAsp(DET) or PEG-PAsp(DET) at N/P ratio of 20, and other groups of rats were treated with micelle solutions (N/P = 20) in the same manner. These animals were killed at 2 and 3 days after administration (n = 4-5), and luciferase activity was measured.

In vivo uptake of polyplex micelles

To evaluate in vivo uptake of polyplex micelles in the carotid artery with neointima, Cy3-pDNA was complexed with cRGD-PEG-PAsp(DET) or PEG-PAsp(DET) at N/P ratio of 5. The rats were subjected to balloon injury, and 21 days later, 200 μL of each micelle solution (20 mg pDNA / mL) was administered to the neointima-induced carotid artery in the same manner (n = 3). At 1 day after administration, the carotid arteries were excised, and frozen sections (4 μm thick) were cut out. Cross sections of the arteries were analyzed by means of a fluorescent digital microscope (BZ-8000, Keyence, Osaka, Japan) with a suitable filter set. Briefly, the ring-shaped arterial cross section was radially divided into five parts, and a fluorescent photomicrograph of each part was acquired as digital data. The fluorescence intensity in the neointima was quantified as pixel number ($Pix_{neointima}$), using image analysis software (WinROOF, Mitani Corporation, Fukui, Japan). Since the elastic laminae of the medial layer possessed weak autonomous fluorescence, the pixel number of the elastic laminae was also quantified ($Pix_{eleastic}$), and the fluorescence intensity of the neointima was standardized

as follows:

Fluorescence intensity index = $Pix_{neointima}$ / $Pix_{eleastic}$

The mean fluorescence intensity indexes of five parts were used as the value of each cross section.

Statistical analysis

All values are shown as mean ± S.E.M. Statistical significance was determined by two-sided Mann-Whitney's U test. Differences with $P < 0.05$ were considered significant.

Acknowledgements

This work was supported by Special Coordination Funds for Promoting Science and Technology from the Ministry of Education, Culture, Sports, Science and Technology (MEXT), and the Core Research Program for Educational Science and Technology (CREST) from the Japan Science and Technology Corporation (JST). We are especially grateful to Mr Noboru Sunaga, Ms Junko Kawakita, and Ms Takae Shimada for their technical supports.

Conflict of interest

The authors declare no conflict of interest.

References

1. Taniyama Y, Tachibana K, Hiraoka K, Namba T, Yamasaki K, Hashiya N et al. Local delivery of plasmid DNA into rat carotid artery using ultrasound. *Circulation* 2002; **105**: 1233-1239.
2. Nishikage S, Koyama H, Miyata T, Ishii S, Hamada H, Shigematsu H. *In vitro* electroporation enhances plasmid-based gene transfer of basic fibroblast growth factor for the treatment of ischemic limb. *J Surg Res* 2004; **120**: 37-46.
3. Tomanin R, Scarpa M. Why do we need new gene therapy viral vectors? Characteristics, limitations and future perspectives of viral vector transduction. *Curr Gene Ther* 2004; **4**: 357-372.
4. Edelstein ML, Abedi MR, Wixon J. Gene therapy clinical trials worldwide to 2007—an update. *J Gene Med* 2007; **10**: 833-842.
5. Pack, DW, Hoffman AS, Pun S, Stayton PS. Design and development of polymers for gene delivery. *Nat Rev Drug Discovery* 2005; **4**: 581-593.
6. Mastrobattista E, van der Aa MA, Hennink WE, Crommelin DJA. Artificial viruses: a nanotechnological approach to gene delivery. *Nat Rev Drug Discovery* 2006; **5**: 115-121.
7. Wagner E, Ogris M, Zauner W. Polysine-based transfection systems utilizing receptor-mediated delivery. *Adv Drug Deliv Rev* 1998; **30**: 97-113.
8. Oupicky D, Konak C, Ulbrich K, Wolfert MA, Seymour LW. DNA delivery systems based on complexes of DNA with synthetic polycations and their copolymers. *J Control Release* 2000; **65**: 149-171.
9. Pedroso de Lima MC, Simoes S, Pires P, Faneca H, Duzgunes N. Cationic lipid-DNA complexes in gene delivery: from biophysics to biological applications. *Adv Drug Delivery Rev* 2001; **47**: 277-294.
10. Merdan T, Kopecek J, Kissel T. Prospects for cationic polymers in gene and oligonucleotide therapy against cancer. *Adv Drug Delivery Rev* 2002; **54**: 715-758.
11. Ogris M, Brunner S, Schuller S, Kircheis R, Wagner E. PEGylated DNA/transfection-PEI complexes: reduced interaction with blood components, extended circulation in blood and potential for systemic gene delivery. *Gene Ther* 1999; **6**: 595-605.
12. Oupicky D, Konak D, Dash PR, Seymour LW, Ulbrich K. Effect of albumin and polyanion on the structure of DNA complexes with polycation containing hydrophilic nonionic block. *Bioconjug Chem* 1999; **10**: 764-772.

13. Kakizawa Y, Kataoka K. Block copolymer micelles for delivery of gene and related compounds. *Adv Drug Delivery Rev* 2002; **54:** 203-222.
14. Katayose S, Kartaoka K. Water-solubule polyion complex association of DNA and poly(ethylene glycol)-poly(L-lysine) block copolymer. *Bioconjug Chem* 1997; **8**: 702-707.
15. Osada K, Kataoka K. Drug and gene delivery based on supramolecular assembly of PEG-polypeptide hybrid block copolymers. *Adv Polym Sci* 2006; **202**: 113-153.
16. Itaka K, Harada A, Nakamura K, Kawaguchi H, Kataoka K. Evaluation by fluorescence resonance energy transfer of the stability of nonviral gene delivery vectors under physiological conditions. *Biomacromolecules* 2002; **3**: 841-845.
17. Harada-Shiba M, Yamauchi K, Harada A, Takamizawa I, Shimokado K, Kataoka K. Polyion complex micelles as vectors in gene therapy-pharmakokinetics and *in vivo* gene transfer. *Gene Ther* 2002; **9**: 407-414.
18. Itaka K, Yamanouchi K, Harada A, Nakamura K, Kawaguchi H, Kataoka K. Polyion complex micelles from plasmid DNA and poly(ethylene glycol)-poly(L-lysine) block copolymer as serum-tolerable polyplex system: physicochemical properties of micelles relevant to gene transfection efficiency. *Biomaterials* 2003; **24**: 4495-4506.
19. Han M, Bae Y, Nishiyama N, Miyata K, Oba M, Kataoka K. Transfection study using multicellular tumor spheroids for screening non-viral polymeric gene vectors with low cytotoxicity and high transfection efficiencies. *J Control Release* 2007; **121**: 38-48.
20. Akagi D, Oba M, koyama H, Nishiyama N, Fukushima S, Miyata T et al. Biocompatible micellar nanovectors achieve efficient gene transfer to vascular lesions without cytotoxicity and thrombus formation. *Gene Ther* 2007; **14**: 1029-1038.
21. Kanayama N, Fukushima S, Nishiyama N, Itaka K, Jang W-D, Miyata K et al. A PEG-based biocompatible block catiomer with high buffering capacity for the construction of polyplex micelles showing efficient gene transfer toward primary cells. *ChemMedChem* 2006; **1**: 439-444.
22. Itaka K, Ishii T, Hasegawa Y, Kataoka K. Biodegradable polyamino acid-based polycations as safe and effective gene carrier minimizing cumulative toxicity. *Biomaterials* 2010; **31**: 3707-3714.
23. Miyata K, Oba M, Nakanishi M, Fukushima S, Yamasaki Y, Koyama H et al. Polyplexes from poly(aspartamide) bearing 1,2-diaminoethane side chains induce pH-selective, endosomal membrane destabilization with amplified transfection and negligible cytotoxicity. *J Am Chem Soc* 2008; **130**: 16287-16294.

24. Wakebayashi D, Nishiyama N, Yamasaki Y, Itaka K, Kanayama N, Harada A et al. Lactose-conjugated polyion complex micelles incorporating plasmid DNA as a targetable gene vector system: their preparation and gene transfecting efficiency against cultured HepG2 cells. *J Control Release* 2004; **95**: 653-664.
25. Suh W, Han SO, Yu L, Kim SW. An angiogenic endothelial-cell-targeted polymeric gene carrier. *Mol Ther* 2002; **6**: 664-672.
26. Ogris M, Walker G, Blessing T, Kircheis R, Wolschek M, Wagner E. Tumor-targeted gene therapy: strategies for the preparation of ligand-polyethylene glycol-polyethylenimine / DNA complexes. *J Control Release* 2003; **91**: 173-181.
27. Haubner R, Gratias R, Diefenbach B, Goodman SL, Jonczyk A, Kessler H. Structural and functional aspects of RGD-containing cyclic pentapeptides as highly potent and selective integrin αvβ3 antagonist. *J Am Chem Soc* 1996; **118**: 7461-7472.
28. Brooks PC, Clark RAF, Cheresh DA. Requirement of vascular integrin αvβ3 for angiogenesis. *Science* 1994; **264**: 569-571.
29. Kim WJ, Yockman JW, Lee M, Jeong JH, Kim YH, Kim SW. Soluble *Flt-1* gene delivery using PEI-*g*-PEG-RGD conjugate for anti-angiogenesis. *J Control Release* 2005; **106**: 224-234.
30. Kim WJ, Yockman JW, Jeong JH, Christensen LV, Lee M, Kim YH et al. Anti-angiogenic inhibition of tumor growth by systemic delivery of PEI-*g*-PEG-RGD/pCMV-sFlt-1 complexes in tumor-bearing mice. *J Control Release* 2006; **114**: 381-388.
31. Choi ET, Engel L, Callow AD, Sun S, Trachtenberg J, Santoro S et al. Inhibition of neointimal hyperplasia by blocking alpha V beta 3 integrin with a small peptide antagonist GpenGRGDSPCA. *J Vasc Surg* 1994; **19**: 125-134.
32. Hoshiga M, Alpers CE, Smith LL, Giachelli CM, Schwartz SM. Alpha-v beta-3 integrin expression in normal and atherosclerotic artery. *Circ Res* 1995; **77**: 1129-1135.
33. van der Zee R, Murohara T, Passeri J, Kearney M, Cheresh DA, Isner JM. Reduced intimal thickening following alpha(v)beta3 blockade is associated with smooth muscle cell apoptosis. *Cell Adhes Common* 1998; **6**: 371-379.
34. Srivatsa SS, Fitzpatrick LA, Tsao PW, Reilly TM, Holmes DR Jr, Schwartz RS et al. Selective alpha v beta 3 integrin blockade potently limits neointimal hyperplasia and lumen stenosis following deep coronary arterial stent injury: evidence for the functional importance of integrin alpha v beta 3 and osteopontin expression during neointima formation. *Cardiovasc Res* 1997; **36**: 408-428.

35. Kokudo T, Uchida H, Choi ET. Integrin αvβ3 as a target in the prevention of neointimal hyperplasia. *J Vasc Surg* 2007; **45**: 33-38.
36. Oba M, Fukushima S, Kanayama N, Aoyagi K, Nishiyama N, Koyama H et al. Cyclic RGD peptide-conjugated polyplex micelles as a targetable gene delivery system directed to cells possessing αvβ3 and αvβ5 integrins. *Bioconjugate Chem* 2007; **18**: 1415-1423.
37. Oba M, Aoyagi K, Miyata K, Matsumoto Y, Itaka K, Nishiyama N et al. Polyplex micelles with cyclic RGD peptide ligands and disulfide cross-links directing to the enhanced transfection via controlled intracellular trafficking. *Mol Pharm* 2008; **5**: 1080-1092.
38. Grosse S, Aron Y, Thevenot G, Francosis D, Monsigny M, Fajac I. Potocytosis and cellular exit of complexes as cellular pathway for gene delivery by polycations. *J Gene Med* 2005; **7**: 1275-1286.
39. Wickman TJ, Filardo EJ, Cheresh DA, Nemerow GR. Integrin αvβ5 selectively promotes adenovirus mediated cell membrane permeabilization. *J Cell Biol* 1994; **127**: 257-264.
40. Wary KK, Mainiero F, Isakoff SJ, Marcantonio EE, Giancotti FG. The adaptor protein Shc couples a class of integrin to the control of cell cycle progression. *Cell* 1996; **87**: 733-743.
41. Wary KK, Mariotti A, Zurzolo C, Giancotti FG. A requirement for caveolin-1 and associated kinase Fyn in integrin signaling and anchorage-dependent cell growth. *Cell* 1998; **94**: 625-634.
42. Marinelli L, Gottschalk KE, Meyer A, Novellino E, Kessler H. Human integrin αvβ5: homology modeling and ligand binding. *J Med Chem* 2004; **47**: 4166-4177.
43. Stary HC, Blankenhorn DH, Chandler AB, Glagov S, Insull Jr W, Richardson M et al. A definition of the intima of human arteries and of its atherosclerosis-prone regions. A report from the Committee on Vascular Lesions of the Council on Arteriosclerosis, American Heart Association. *Circulation* 1992; **85**: 391-405.
44. Guzman RJ, Lemarchand P, Crystal RG, Epstein SE, Finkel T. Efficient and selsective adenovirus-mediated gene transfer into vascular neointima. *Circulation* 1993; **88**: 2838-2848.
45. Pelkmans L, Kartenbeck J, Helenius A. Caveolar endocytosis of simian virus 40 reveals a new two-step vesicular transport pathway to the ER. *Nat Cell Biol* 2001; **3**: 473-483.

Figure legends

Figure 1. (a) Chemical structure of cRGD-PEG-PAsp(DET) block copolymer. (b) Schematic illustration of polyplex micelle formation through electrostatic forces.

Figure 2. Flow cytometric analysis of integrin expression on HUVEC (a) and VSMC (b). FITC-labeled antibodies against αvβ3 integrin (blue), αvβ5 integrin (red), or mouse IgG (black) was added to each cell suspension, followed by incubation on ice in the dark.

Figure 3. Effect of luciferase gene expression in vitro. HUVEC (a) and VSMC (b) were transfected with cRGD-PEG-PAsp(DET) and PEG-PAsp(DET) micelles prepared at various N/P ratios. Gene expression was assessed by measuring luciferase activity 24 hours later. Data are mean±S.E.M. (* $P < 0.05$).

Figure 4. Cellular uptake of polyplex micelles (N/P=5). cRGD-PEG-PAsp(DET) micelles with N/P ratio of 5 loaded with Cy5-labeled pDNA were applied to HUVEC (a) and VSMC (b) for various incubation times. PEG-PAsp(DET) micelles containing Cy5-pDNA were used as control. Mean fluorescence intensity at each incubation time was assessed. Data are mean±S.E.M. (*$P < 0.05$, **$P < 0.01$)

Figure 5. Intracellular distribution of pDNA challenged by polyplex micelles. cRGD-PEG-PAsp(DET) and PEG-PAsp(DET) micelles loaded with Cy5-labeled pDNA (red) were incubated with HUVEC (a, b) and VSMC (e, f) for 6 and 24 hours. Confocal laser scanning observation was performed using a 63× objective. The acidic endosomes and lysosomes were stained with LysoTracker Green (green), and the lipid rafts and caveosomes were stained with CT-B Alexa Fluor 488 (green). The rate of colocalization of Cy5-pDNA with LysoTracker Green or CT-BAlexa Fluor 488 was quantified (c, d, g, h). Data are mean ±S.E.M. RGD(-) = PEG-PAsp(DET) micelles. RGD(+) = cRGD-PEG-PAsp(DET) micelles.

Figure 6. In vivo gene expression evaluated from luciferase activity after intra-arterial delivery of c RGD-PEG-PAsp(DET) and PEG-PAsp(DET) micelles at N/P ratios of 5 (a) and 20 (b, c). Each polymer was complexed with pCAccluc+ and instilled into rat carotid artery with neointima. At 1, 2, 3 and 4 days (a), and at 2 and 3 days (b, c), the

common carotid artery was excised and luciferase activity was measured. Values are expressed as RLU / mg protein. Values are shown as mean ±S.E.M (*$P < 0.05$, **P < 0.01). RGD(-) = PEG-PAsp(DET) micelles. RGD(+) = cRGD-PEG-PAsp(DET) micelles.

Figure 7. Photomicrographs of rat carotid artery transfected with polyplex micelles composed of Cy3-labeled pCAccluc+ and cRGD-PEG-PAsp(DET) at N/P ratio of 5 (a) and composed of Cy3-labeled pCAccluc+ and PEG-PAsp(DET) as control (b). Mean fluorescence intensity index in neointima of each section. Values are shown as mean±S.E.M (c). Representative photomicrograph of rat carotid artery with hematoxylin-eosin staining (d). RGD(-) = PEG-PAsp(DET) micelles. RGD(+) = cRGD-PEG-PAsp(DET) micelles. L, lumen; I, intima; M; media; A; adventitia.

a

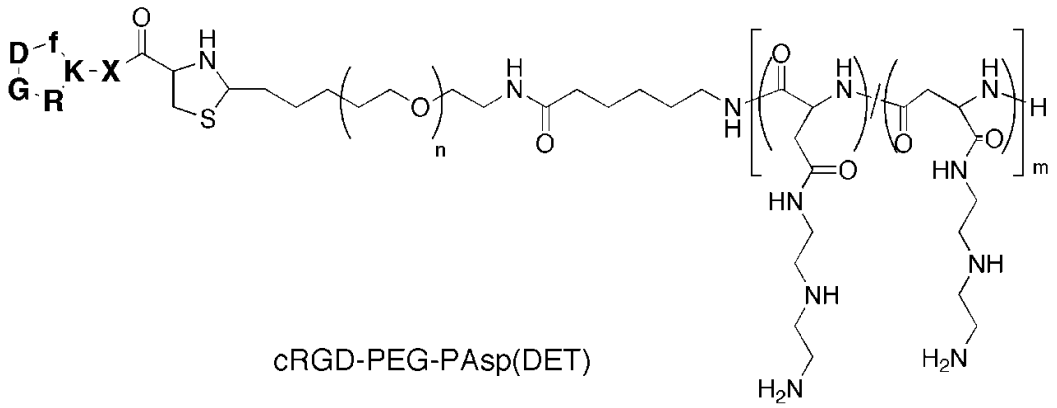
cRGD-PEG-PAsp(DET)

b

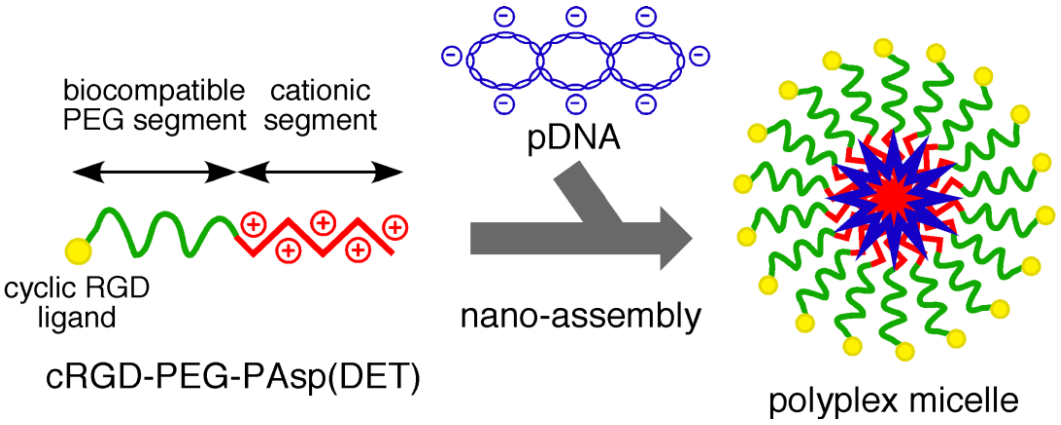
biocompatible PEG segment
cationic segment
cyclic RGD ligand
cRGD-PEG-PAsp(DET)
pDNA
nano-assembly
polyplex micelle

Figure 1

a

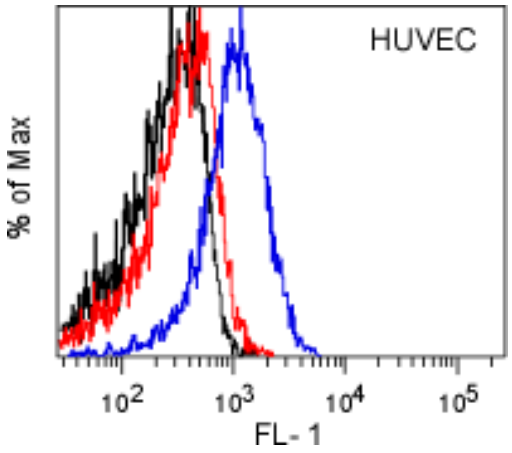

b

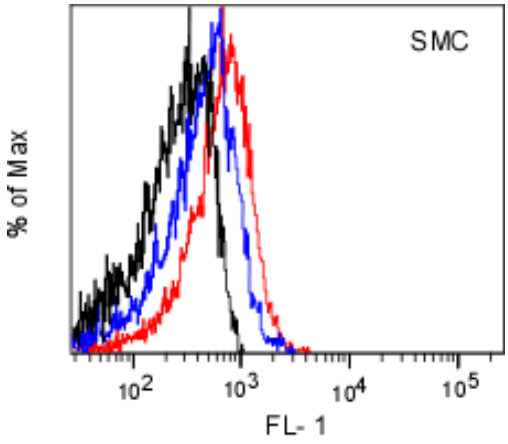

Figure 2

a

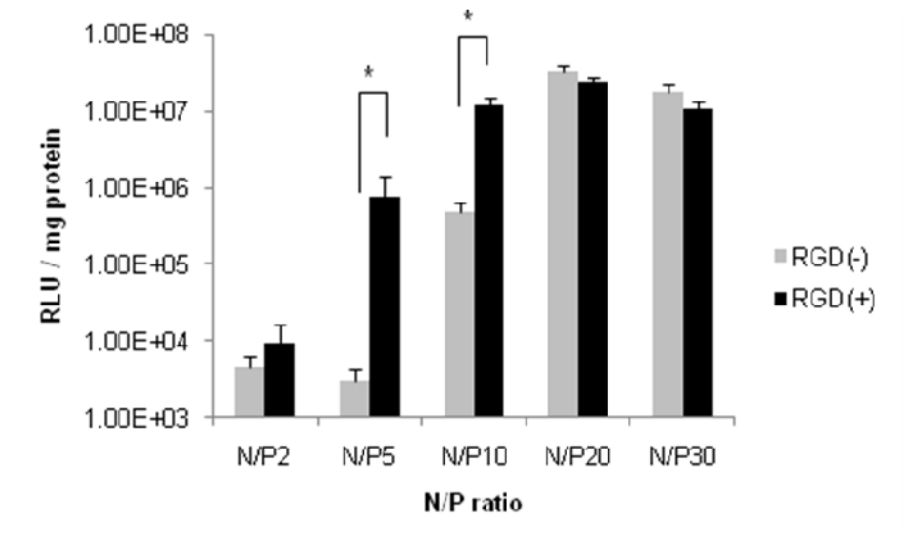
1.00E+08
1.00E+07
1.00E+06
1.00E+05
1.00E+04
1.00E+03
RLU / mg protein
*
*
N/P2
N/P5
N/P10
N/P20
N/P30
N/P ratio
RGD(-)
RGD(+)

b

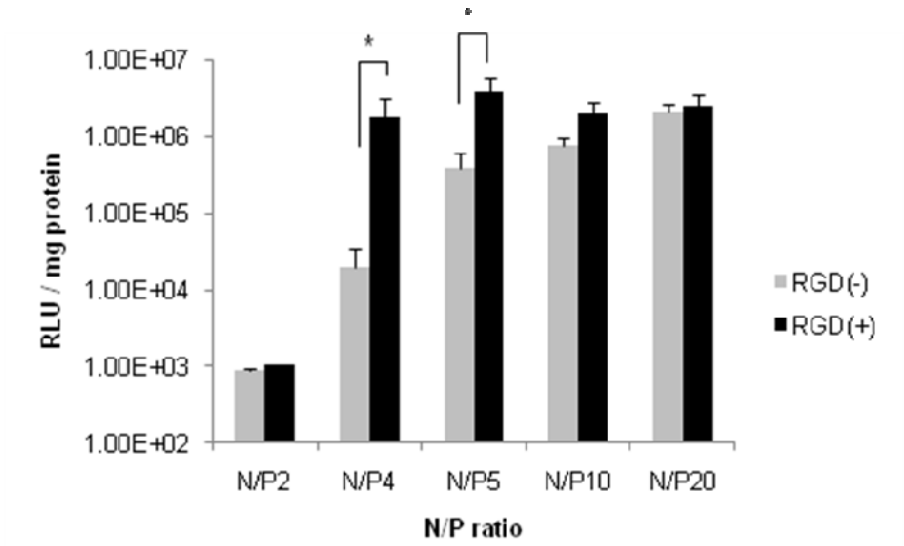
1.00E+07
1.00E+06
1.00E+05
1.00E+04
1.00E+03
1.00E+02
RLU / mg protein
*
*
N/P2
N/P4
N/P5
N/P10
N/P20
N/P ratio
RGD(-)
RGD(+)

Figure 3

a

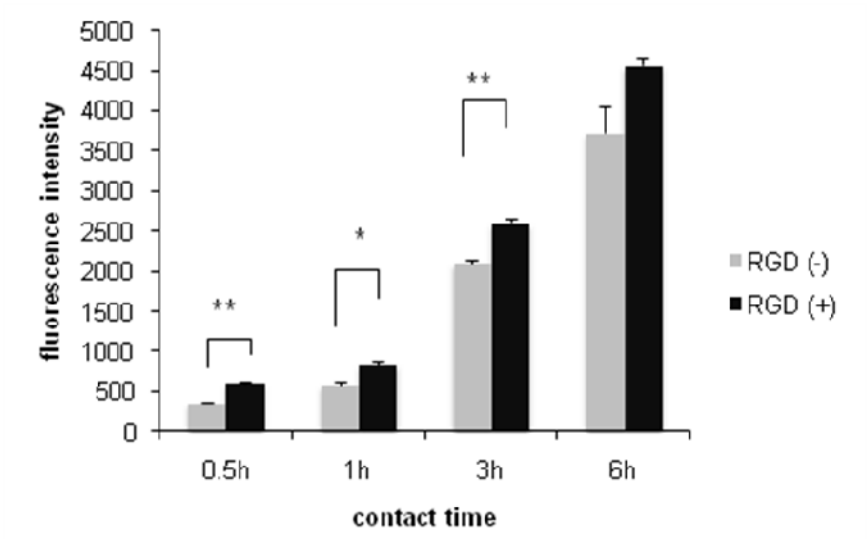
5000
4500
4000
3500
3000
2500
2000
1500
1000
500
0
fluorescence intensity
**
*
**
0.5h
1h
3h
6h
contact time
RGD (-)
RGD (+)

b

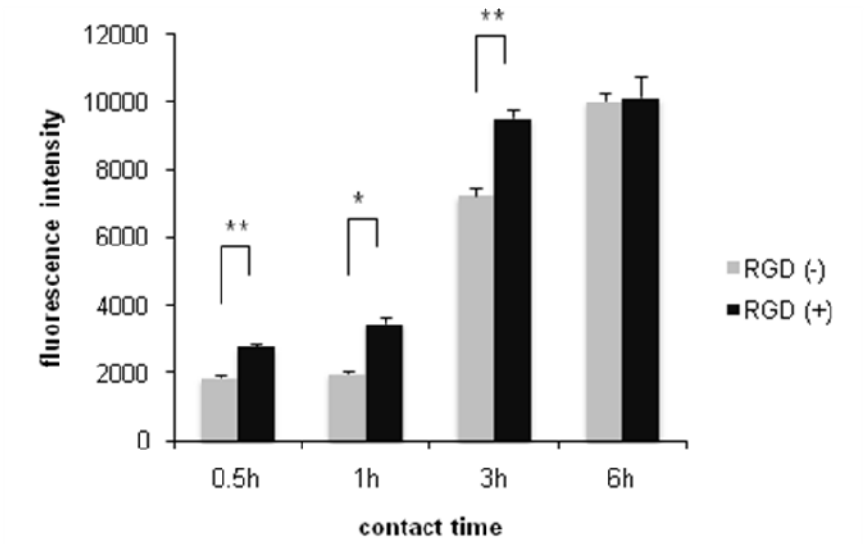
12000
10000
8000
6000
4000
2000
0
fluorescence intensity
**
*
**
0.5h
1h
3h
6h
contact time
RGD (-)
RGD (+)

Figure 4

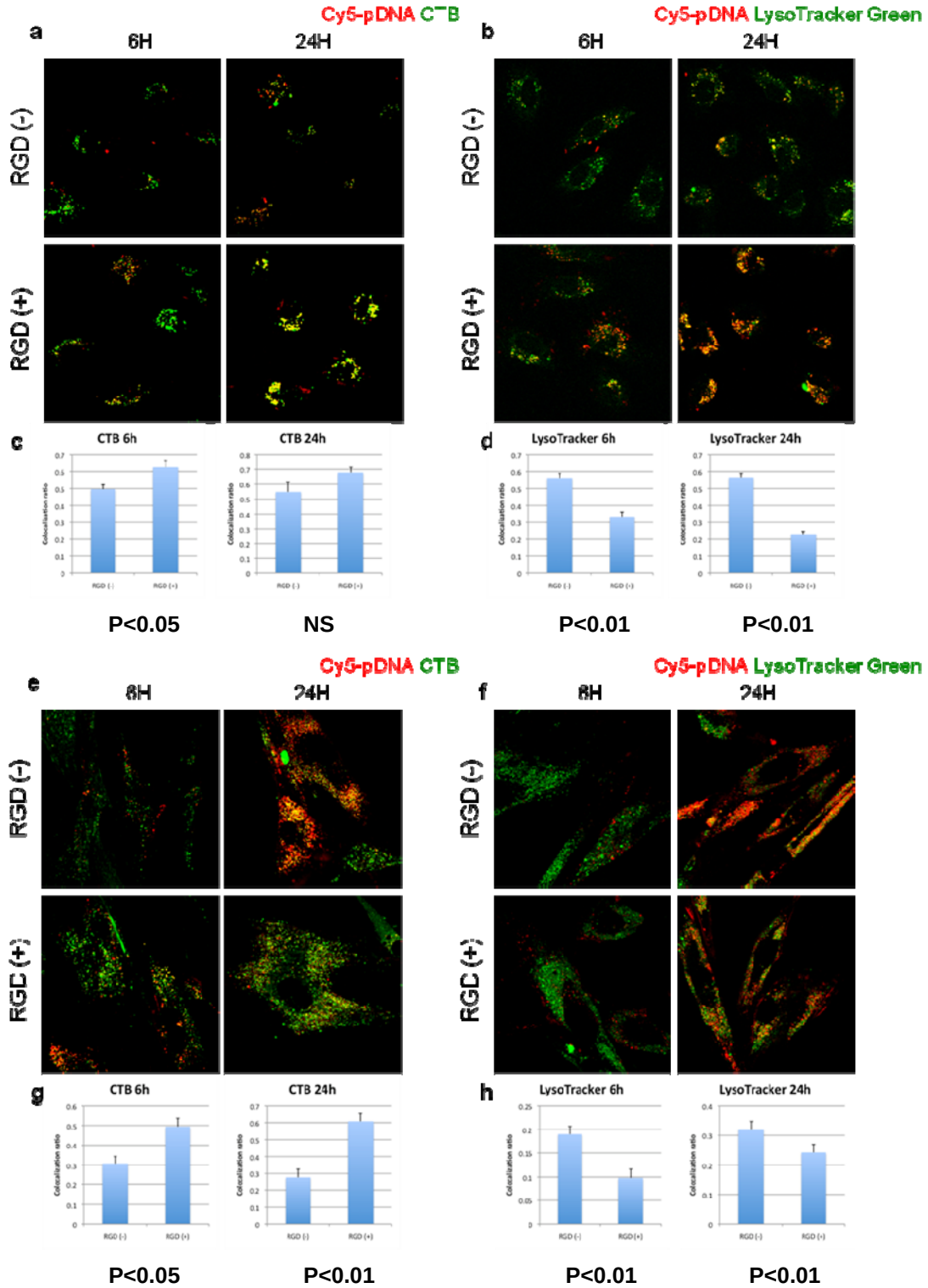
Cy5-pDNA CTB
Cy5-pDNA LysoTracker Green
a
6H
24H
RGD (-)
RGD (+)
b
6H
24H
RGD (-)
RGD (+)
c
CTB 6h
CTB 24h
d
LysoTracker 6h
LysoTracker 24h
P<0.05
NS
P<0.01
P<0.01
Cy5-pDNA CTB
Cy5-pDNA LysoTracker Green
e
6H
24H
RGD (-)
RGD (+)
f
6H
24H
RGD (-)
RGD (+)
g
CTB 6h
CTB 24h
h
LysoTracker 6h
LysoTracker 24h
P<0.05
P<0.01
P<0.01
P<0.01

Figure 5

a

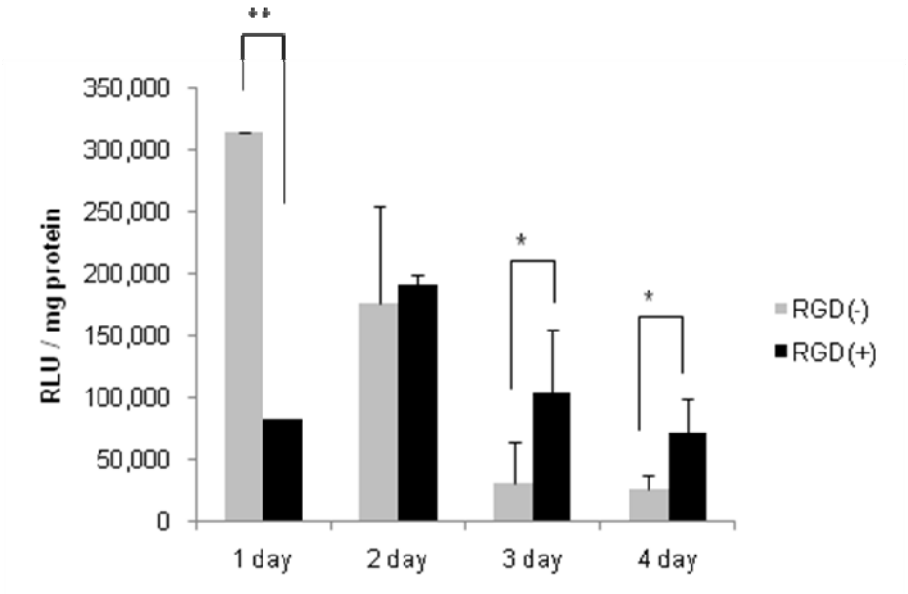
**
*
*
350,000
300,000
250,000
200,000
150,000
100,000
50,000
0
RLU / mg protein
1 day
2 day
3 day
4 day
RGD(-)
RGD(+)

b

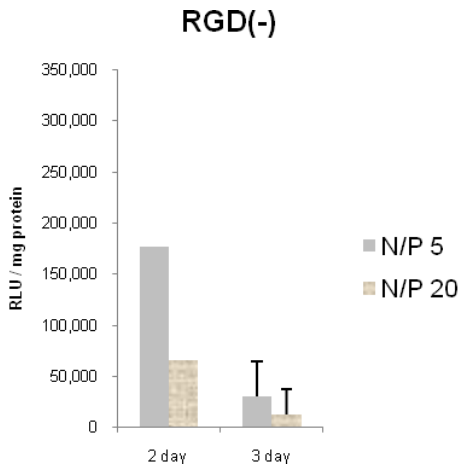
RGD(-)
350,000
300,000
250,000
200,000
150,000
100,000
50,000
0
RLU / mg protein
2 day
3 day
N/P 5
N/P 20

c

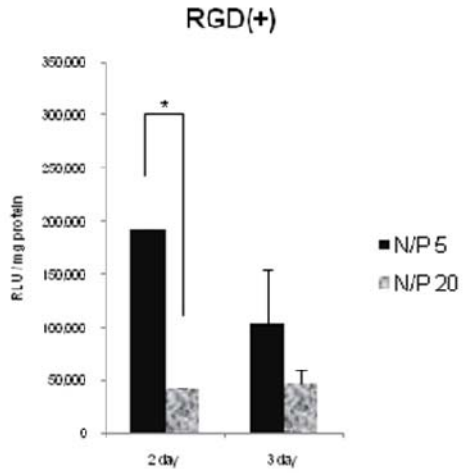
RGD(+)
*
RLU / mg protein
2 day
3 day
N/P 5
N/P 20

Figure 6

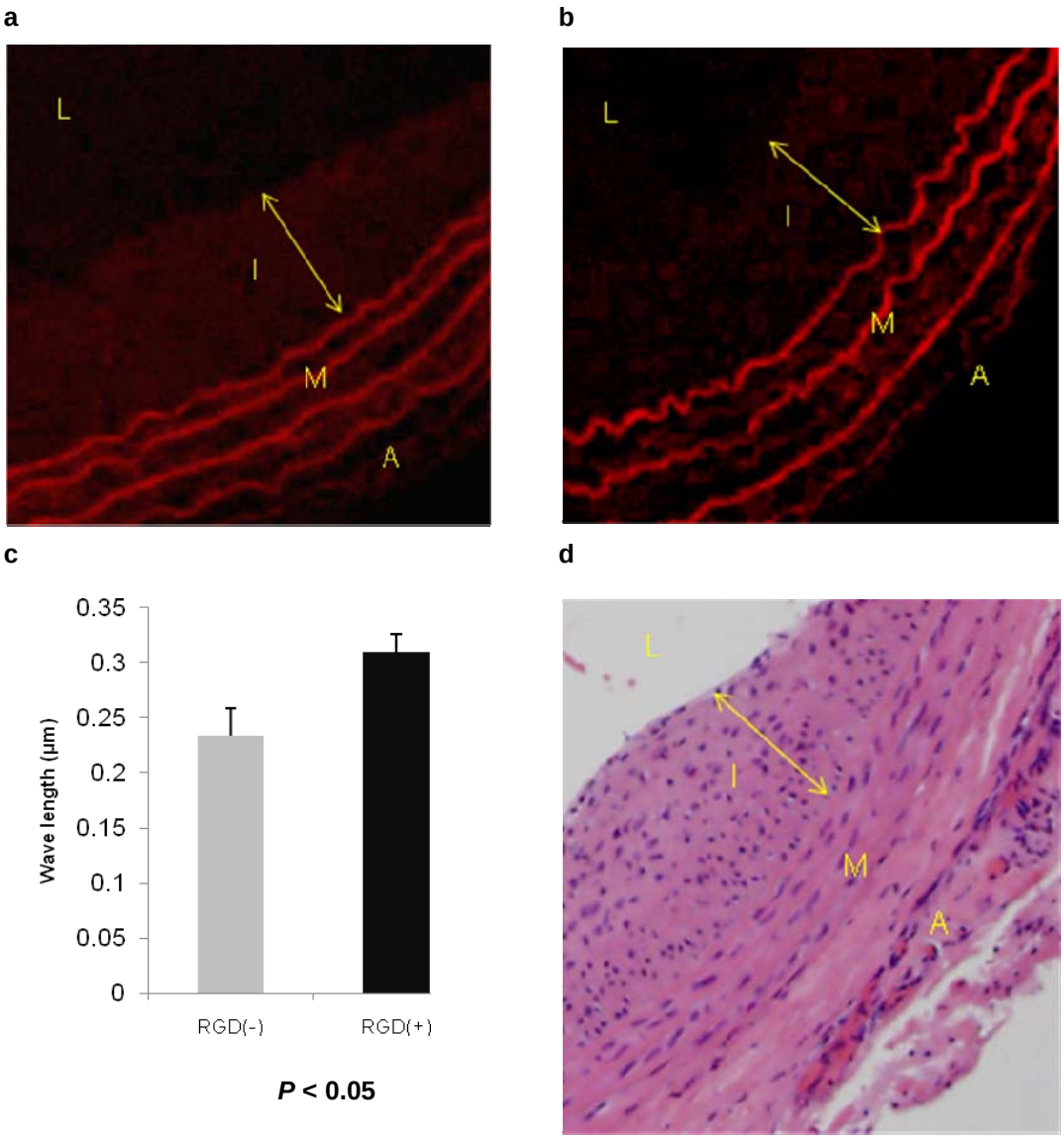
a
b
L
I
M
A
L
I
M
A
c
d
0.35
0.3
0.25
0.2
0.15
0.1
0.05
0
Wave length (μm)
RGD(-)
RGD(+)
P < 0.05
L
I
M
A

Figure 7